

Journal of Composite Materials

<http://jcm.sagepub.com/>

Processing and characterization of 100% hemp-based biocomposites obtained by vacuum infusion

G Francucci, NW Manthey, F Cardona and T Aravinthan

Journal of Composite Materials 2014 48: 1323 originally published online 3 May 2013

DOI: 10.1177/0021998313485266

The online version of this article can be found at:

<http://jcm.sagepub.com/content/48/11/1323>

Published by:



<http://www.sagepublications.com>

On behalf of:



American Society for Composites

Additional services and information for *Journal of Composite Materials* can be found at:

Email Alerts: <http://jcm.sagepub.com/cgi/alerts>

Subscriptions: <http://jcm.sagepub.com/subscriptions>

Reprints: <http://www.sagepub.com/journalsReprints.nav>

Permissions: <http://www.sagepub.com/journalsPermissions.nav>

Citations: <http://jcm.sagepub.com/content/48/11/1323.refs.html>

>> [Version of Record](#) - Apr 25, 2014

[OnlineFirst Version of Record](#) - May 3, 2013

[What is This?](#)

Processing and characterization of 100% hemp-based biocomposites obtained by vacuum infusion

G Francucci^{1,2}, NW Manthey¹, F Cardona¹ and T Aravinthan¹

Abstract

Novel biocomposites made of an acrylated epoxidized hemp oil based bioresin reinforced with random hemp fiber mat were manufactured by the vacuum infusion technique. Mechanical properties (tensile, flexural, Charpy impact and interlaminar shear), dynamic mechanical properties (glass transition temperature, storage modulus and crosslink density) and moisture absorption properties (saturation moisture level and diffusion coefficient) were investigated and compared with samples manufactured under the same conditions but using a commercial synthetic vinylester resin as the polymeric matrix. Results showed that the 100% biocomposites mechanical performance is comparable to that of the hybrid composites made with the synthetic resin. Moisture absorption tests showed that acrylated epoxidized hemp oil based samples displayed both higher diffusion coefficient and saturation moisture content; however, fiber reinforcement was the dominant transfer mechanism. Vinyl ester based samples were found to have higher storage modulus, glass transition temperature and crosslink density than acrylated epoxidized hemp oil samples.

Keywords

Biocomposite, dynamic mechanical analysis, mechanical properties, moisture absorption, natural fibers

Introduction

The high environmental impact caused by traditional composite materials made with petroleum-based polymeric resins and synthetic fibers (glass, carbon, aramid) has encouraged the development of biocomposites to replace those materials predominately in non-structural applications. Although some biocomposites are being created using natural fibers reinforcing petrochemical matrices (they might be called hybrid composites), the best case scenario from the environmental point of view is to produce composites in which both matrix and reinforcement are derived from natural resources. These materials have environmental advantages over petroleum-based materials, since they are made from bio-degradable and/or renewable resources.¹ Plant-based natural fibers and resins also help reduce the carbon footprint of the end composite from the growing of the plants and enhanced energy recovery at the end of their lifecycle.²

It is understood that the performance of biocomposites is lower than that of traditional composites.

Water absorption^{3,4} can result in swelling of the fibers, negatively influence the dimensional stability of the natural fiber composites and also deteriorate the mechanical properties of the fibers and the composite due to weakening of the matrix–fiber interface. The effect of water and moisture absorption of natural fiber plastic composites is a serious concern, especially for outdoors applications, and was studied by numerous authors.^{5–17} Moreover, the adhesion between natural fibers and the polymeric matrix is often

¹Centre of Excellence in Engineered Fibre Composites (CEEFC), University of Southern Queensland, Toowoomba, Queensland, Australia

²Composite Materials Group, Research Institute of Material Science and Technology (INTEMA-CONICET), Materials Engineering Department, Engineering Faculty, National University of Mar del Plata, Mar del Plata, Argentina

Corresponding author:

NW Manthey, Centre of Excellence in Engineered Fibre Composites (CEEFC), University of Southern Queensland, Toowoomba, West St, Darling Heights QLD 4350, Queensland, Australia.
Email: nathan.manthey@usq.edu.au

insufficient, resulting in low mechanical properties of the composites. In addition, plant-based fibers suffer lignocellulosic degradation at low temperatures (around 200°C), limiting their applications and processing temperatures.¹⁸ For this reason many researchers have tried to improve the fiber–matrix interface and decrease natural fiber moisture uptake. Bledzki and Gassan⁷ made an extensive review on the most used methods for surface modification of natural fibers. They sorted the treatments as chemical or physical methods. Usually, chemical methods bring about an active surface by introducing some reactive groups, and provide the fibers with higher extensibility through partial removal of lignin and hemicelluloses,¹⁹ while physical methods change structural and surface properties of the fiber and thereby influencing mechanical bonding to polymers.

Most of the treatments are performed to improve compatibility of natural fibers with petrochemical resins. However, if bioresins are used and in particular bioresins derived from the same plant which the fibers were extracted from, the compatibility may be improved. Therefore, this work studies the performance of 100% hemp-based biocomposites made with an acrylated epoxidized hemp oil (AEHO) based bioresin reinforced with untreated hemp fiber random mat and compares it to that of hybrid composites made with vinyl ester (VE) resin reinforced with the same hemp fiber mat. To our knowledge, the properties and performance of this particular biocomposite have not been characterized yet in literature. Mechanical properties (tensile, flexural, Charpy impact and interlaminar shear), dynamic mechanical properties (glass transition temperature, storage modulus and crosslink density) and water absorption properties (saturation moisture level and diffusion coefficient) were investigated.

Liquid composite molding (LCM) techniques, such as resin transfer molding (RTM) or vacuum infusion (VI) seem to be a good choice for processing natural fiber composites. They make it possible to obtain high quality laminates, repeatability, high surface finish and dimensional tolerances and because of the low processing temperatures, fibers do not suffer thermo-mechanical degradation as in some thermoplastic processing techniques. In LCM techniques a catalyzed resin is forced through a mold, which contains the dry reinforcement. In RTM, the preform (a stack of several layers of the fabric used as reinforcement) is compacted between two rigid mold faces. In VI a flexible vacuum bag is used as the upper part of the mold. In this work, VI was used to manufacture the biocomposite panels due to the lower tooling cost required. The main disadvantages of this technique are that it does not allow constant thickness along the panel and high surface finish in both sides of the part to be obtained.

Materials

AEHO as synthesized according to our previous publications and containing 4.1 acrylate and hydroxyl groups per triglyceride was used as the base bioresin.^{20,21} AEHO was obtained by the acrylation of the EHO obtained in previous works.^{22,23} A solution of EHO, hydroquinone inhibitor (0.0033 g/mL of EHO + acrylic acid) and AMC-2 catalyst (1.75% by weight of EHO + acrylic acid) were added to a Mettler Toledo LabMax automatic reactor. The reactor comprised a 4-L four-necked reaction vessel equipped with a mechanical ‘ship anchor’ stirrer and thermometer. Stirring was initiated and the reactor temperature was increased until the mixture reached 50°C. The mixture was left at that temperature for 30 min and then the acrylic acid (ACROS Organics) was added in a molar ratio of 1.1 moles per mol of epoxy groups. The exothermic reaction increased the temperature of the mixture rapidly, thus the reactor was set to maintain a constant temperature of 90°C. The reaction was then performed at the mentioned temperature, stirring the mixture at 160 r/min over a period of 12 h. The reaction evolution was monitored by periodic titration of the AEHO/acrylic acid mixture using sodium hydroxide and phenolphthalein as an acid–base indicator. The reaction was considered to be complete when no further changes could be seen in the amount of sodium hydroxide used to neutralize the resin. The expected chemical structure of this resin is shown in Figure 1. FG vinyl ester SPV6003 (FGI Australia) was used as received for the control samples. In the case of the AEHO bioresin, the added styrene comonomer was supplied by Fischer Scientific (UK), the Promoter N2-51 P was sourced from Axon Nobel Ltd and a 40% MEKP based catalyst was used for the curing and sourced from FGI Australia. The Styrene comonomer, promoter and catalyst were all used as received. Short hemp fiber based random mat with a surface density of approximately 730 g/m² was used as the natural fiber reinforcement.

Experimental

Sample preparation

The viscosity of the bioresin after the acrylation process was measured at room temperature (25°C) by means of a Brookfield DV-II+ viscometer, obtaining a value of 20550 CP. This viscosity is too high for most composite processing techniques. Therefore, 33 wt% of styrene was added to the bioresin to decrease its viscosity and make it suitable for manufacturing composite parts by the traditional composite processing techniques. The viscosity after the styrene addition was 358 CP at room temperature. Afterwards, the promoter was

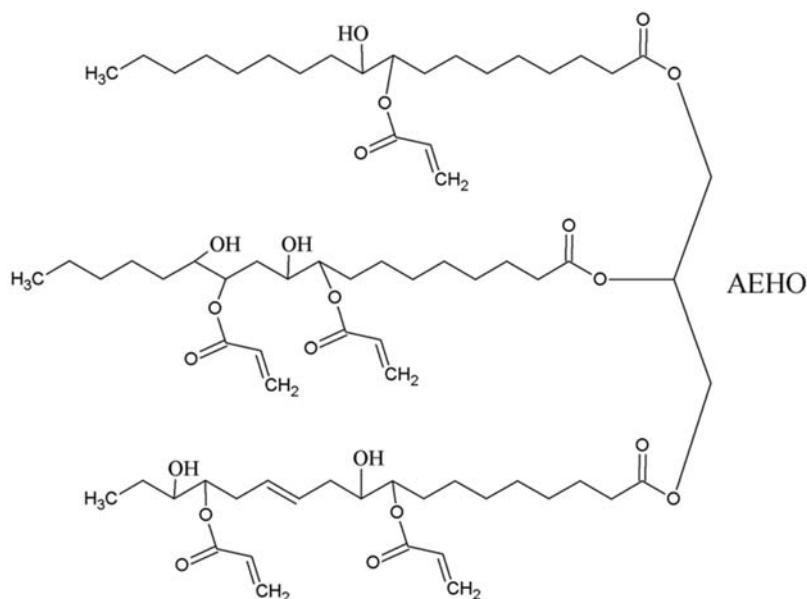


Figure 1. Chemical structure of the AEHO-based bioresin. AEHO: acrylated epoxidized hemp oil.

incorporated to the AEHO/styrene mixture (0.25 wt%) and thoroughly mixed. Subsequent to this the catalyst was added (4 wt%) and stirred thoroughly for several minutes. The resin was degassed under vacuum. For the VE resin system no styrene was added as the system already contains 33 wt% of styrene. Regarding the VE system, 0.25% and 2% promoter and catalyst were used respectively. Neat bioresin and resin samples were also produced by pouring into a waxed glass mold.

Flat biocomposite panels were manufactured by the vacuum infusion technique utilizing two layers of hemp mat reinforcement. These mats were washed with a 2% V/V distilled water and detergent solution to remove contaminants, and then dried at 90°C for 24 h. The manufacture of the composite panels was performed immediately after removing the fiber from the oven in order to prevent moisture absorption and thereby minimize the amount of water present in the natural reinforcement which could lead to void formation and lower mechanical properties of the composites. Both the catalyst and promoter were added to the resin and mixed thoroughly, the mixed resin was degassed and the resin was infused at a vacuum level of 90 kPa. A glass surface was used as the rigid mold face which was thoroughly waxed before every infusion. The flow front was found to be linear with no race tracking, dry spots or fiber washing observed. After the complete impregnation of the reinforcement, the inlet hose was clamped and the resin pressure distribution along the wetted perform was left to stabilize for 2 h. This method

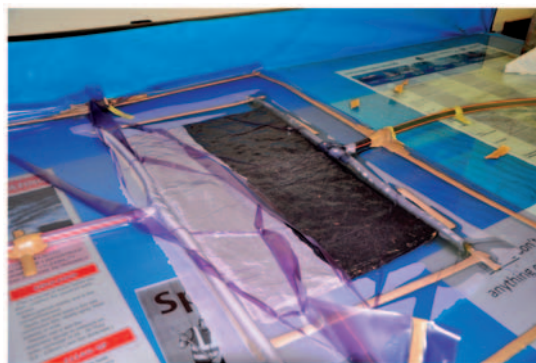


Figure 2. AEHO-based hemp fiber biocomposite undergoing vacuum infusion. AEHO: acrylated epoxidized hemp oil.

helps to remove excess resin and decrease the thickness variations throughout the composite plate.²⁴ Afterwards the outlet hose was clamped and the composite panel was left to cure under vacuum for 24 h at room temperature (~25°C). A 4 h postcuring stage was performed at 80°C for the VE and at 120°C for the bioresin composites respectively to achieve maximum conversion. Figure 2 shows a picture of the biocomposite panel during the infusion.

Although this processing technique does not allow a constant thickness throughout the entire composite plate to be obtained, thickness ranged from 4 to 5 mm, resulting in a fiber volume fraction distribution between 20% and 25%, calculated from equation (1), where n is the number of reinforcement layers stacked

in the preform, β the surface density (g/cm^2), ρ the fiber density (g/cm^3) and t is the preform compressed thickness (or mold cavity thickness) (cm). The cured composite panel thickness was used as the preform compressed thickness and it was taken from an average of several measurements throughout the panel. The fiber density was considered to be $1.4 \text{ g}/\text{cm}^3$, which is an average of the values found in literature ($1.25\text{--}1.5 \text{ g}/\text{cm}^3$).^{25–27} Samples for the mechanical characterization were cut from the manufactured composite plates, dried at 80°C for 4 h to ensure the removal of any induced moisture and then cooled in a desiccator ready for testing. In addition, neat resin samples were produced by pouring the catalyzed resin into a waxed mold, cured as the composite panels and finally cut to size.

$$\text{Fiber Volume Fraction} = \frac{n \cdot \beta}{\rho \cdot t} \quad (1)$$

Scanning electron microscopy

Cross section morphologies of the biocomposite samples were investigated with a JEOL JSM 6460 LV scanning electron microscope (SEM) at National University of Mar Del Plata, Argentina (UNMdP). The fractured surfaces were coated with gold and the samples were scanned at room temperature with an accelerating voltage of 15 kV.

Mechanical testing

Interlaminar shear strength (ILSS) testing was performed to determine the fiber–matrix interfacial shear strength. Testing was performed using ISO 14130 on a MTS Alliance RT/10 10 kN machine with a crosshead speed of 1 mm/min. Charpy impact tests were conducted to determine the impact properties of the biocomposite and hybrid composite samples. Impact properties of the samples were determined using ISO 179 on an Instron Dynatup M14-5162. Charpy impact strength (kJ/m^2) was calculated from equation (2), whereby a_{cU} , h , b an W_B are the Charpy impact strength, thickness, width and the energy at break of the test specimen. Essentially Charpy impact strength corresponds to the energy at break of the specimen divided by the cross-sectional area.

$$a_{cU} = \frac{W_B}{bh} \times 10^3 \quad (2)$$

Flexural testing was conducted to determine the behavior of both neat resin and composite specimens subjected to 3-point simple beam loading. Bioresin and VE flexural properties were obtained through 3-point bending tests conducted in accordance with ISO 178

using a MTS Alliance RT/10 machine. A cross head speed of 2 mm/min and a span/depth ratio of 16:1 were used with specimen dimensions being $80 \times 10 \times 5 \text{ mm}^3$. Biocomposite and hybrid composite flexural properties were measured in accordance with ISO 14125. Tensile tests were conducted in accordance with ISO 527. Tests were performed with a cross-head speed of 2 mm/min using a MTS Insight 100 kN machine. Specimen dimensions were $250 \times 25 \times 5 \text{ mm}^3$. Five specimens of each sample type were used in each mechanical test.

Dynamic mechanical analysis

A calibrated TA Instruments Q800 DMA was used for the dynamic mechanical analysis (DMA). Rectangular specimens with the dimensions $58 \times 10 \times 5 \text{ mm}^3$ were tested in dual cantilever mode. Testing was performed at a temperature ramp of $3^\circ\text{C}/\text{min}$ over a temperature range of approximately $25\text{--}180^\circ\text{C}$. A frequency of 1.0 Hz with an oscillating displacement of $\pm 10 \mu\text{m}$ was also used. Storage modulus (E') and $\tan \delta$ were plotted as a function of temperature by Universal Analysis 2000 version 3.9 A software. Glass transition temperature (T_g) was calculated as the peak of the $\tan \delta$ curve and crosslink density (ν_e) was calculated from the theory of rubber elasticity.²⁸

$$E' = 3\nu_e RT \quad (3)$$

where E' , ν_e , R and T are the storage modulus in the rubbery plateau region ($T_g + 40^\circ\text{C}$), crosslink density, gas constant ($8.314 \text{ J}/(\text{K mol})$) and the absolute temperature in K, respectively.²⁹

Moisture absorption

Moisture absorption tests were performed in order to establish the saturation moisture level and the diffusion coefficient of the samples. Testing was performed in accordance with ASTM D570. Specimens measured $76.2 \times 25.4 \times 5 \text{ mm}^3$ for both neat resin and composite samples. Three specimens of each sample type were used. The specimens were cut to size and the edges were finished with No. 0 sandpaper. After this the specimens were dried at 110°C for 1 h, cooled in a desiccator and weighed to the nearest 0.001 g. The specimens were immersed in distilled water at $23 \pm 1^\circ\text{C}$ and removed at regular intervals, wiped free of surface moisture, immediately weighed to the nearest 0.001 g and then replaced in the water. The following equation was used to calculate the diffusion coefficient.

$$D = \pi \left(\frac{h}{4M_m} \right) m^2 \quad (4)$$

where D , h , M_m and m are diffusion coefficient, thickness of specimen, saturation moisture level and gradient of the linear region from the plot of weight gain against square root of time, respectively.³⁰

Results and discussion

SEM analysis

Figures 3 to 6 show SEM images of the fracture surface of the samples used in the mechanical tests. $300\times$ magnification was used to give a representative image of the overall fiber–matrix behavior whereas $1000\times$ magnification was used to more closely examine individual fiber–matrix interface. It can be seen that fiber pullout

is evident for all sample types. In addition, the gap between the hemp fiber and the AEHO matrix is significantly smaller to the gap observed between the hemp fiber and the VE matrix. This observation suggests that the samples manufactured with VE have the poorest fiber–matrix interface, with the AEHO samples displaying improved fiber–matrix adhesion. It is proposed that the superior fiber–matrix interfacial adhesion of the 100% AEHO-based samples is due to surface chemical compatibility between the natural fibers and the bioresin. It is theorized that the greater quantity of hydroxyl groups present in the AEHO bioresin compared with the VE contributes to enhanced fiber–matrix adhesion. These hydroxyl functional groups present in the AEHO serve to interact with the hydroxyl groups present in the cellulose of the

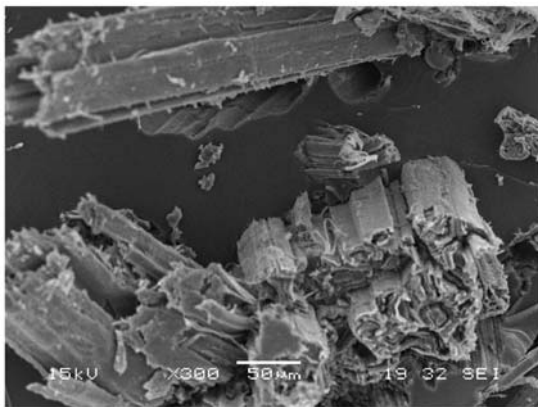


Figure 3. $300\times$ SEM image of hemp fiber/AEHO composite. SEM: scanning electron microscopy; AEHO: acrylated epoxidized hemp oil.

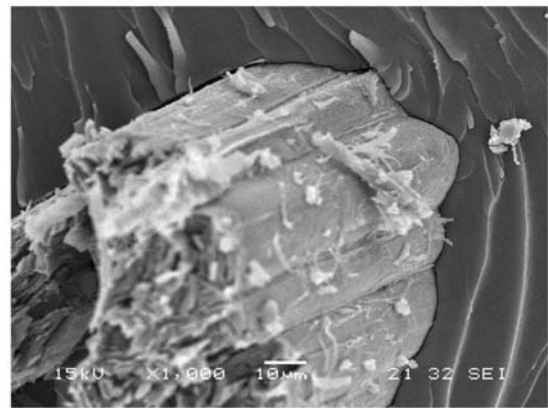


Figure 5. $1000\times$ SEM image of hemp fiber/AEHO composite. SEM: scanning electron microscopy; AEHO: acrylated epoxidized hemp oil.

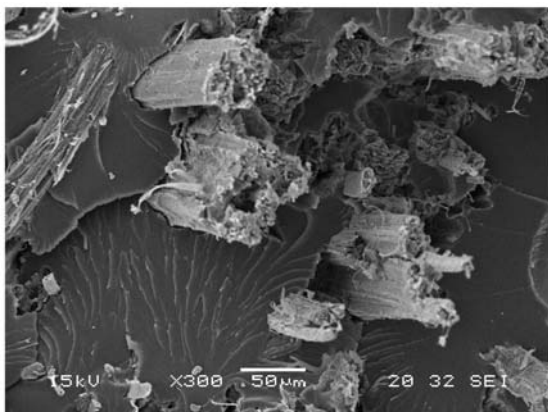


Figure 4. $300\times$ SEM image of hemp fiber/VE composite. SEM: scanning electron microscopy; VE: vinyl ester.



Figure 6. $1000\times$ SEM image of hemp fiber/VE composite. SEM: scanning electron microscopy; VE: vinyl ester.

natural fibers to form strong hydrogen bonds thereby improving adhesion.

Mechanical properties

The interlaminar shear strength of reinforced plastics depends on the fiber–matrix adhesion, resin strength and moisture and void content in the composite.^{31–35} This property has a strong influence on the structural performance of composites, since their strength is strongly influenced by factors weakening the interface. Petker reported that the ILSS increases with the increase in the matrix strength up to certain point whereby the influence of voids becomes increasingly important in the failure mechanism and the ILSS becomes constant despite further increases in resin strength.³⁶

From Figure 7 it is apparent that the interlaminar shear strength of the AEHO/Hemp fiber biocomposites was 47% higher to that of the VE/hemp fiber hybrid composites. During processing, styrene can form bubbles under high vacuum conditions due to its low vapor pressure, and these bubbles can sometimes be trapped in the fabric and remain as voids after the resin cures. However, the same fiber mat and processing conditions were used in the manufacture of the composite panels and the styrene content in the VE resin was the same as in the AEHO. For this reason, void content was almost identical in both composites, and no significant differences in voids size and concentration were observed by SEM among all the samples.

Therefore, the ILSS results suggest that the hemp fiber–AEHO matrix interface is stronger than the hemp fiber–VE interface, since the strength of the VE resin is superior to that of the bioresin. These observations are in accordance to the SEM images showed

previously. As stated before, the higher amount of hydroxyl groups present on the AEHO resin compared with the VE resin could be the reason for the better adhesion between fibers and resin in the biocomposites, since those functional groups interact with the hydroxyl groups present in the cellulose of the natural fibers to form strong hydrogen bonds.

The flexural strength of the samples is shown in Figure 8. VE resin flexural strength was found to be higher than that of the AEHO bioresin. No significant differences could be seen in the value of this property between the biocomposites and the hybrid composites. This is because while the biocomposite was 40% stronger than the bioresin, the strength of the hybrid composite was found to be 40% lower than that of the neat VE resin. This behavior was unexpected, since the tensile strength of hemp fibers (between 310 and 900 MPa)^{37,38} is higher than the strength of the VE resin (86 MPa according to the supplier).

It is theorized that the decrease in flexural strength in this case may be caused by the weak fiber–matrix interfacial adhesion present in the hybrid composites, as observed in the SEM images and the ILSS results. Since the bonding between fibers and matrix is low, the load is not transferred properly from the resin to the fibers and therefore most of the load is withstood by the resin itself. In addition, the empty space between the fibers and the matrix act as flaws in the resin, and they initiate cracks at stresses lower than that of the resin failure stress. Conversely, the biocomposites showed a higher flexural strength than the neat bioresin because the strength of this resin is relatively low and the interface with the hemp fibers is stronger than in the case of the hybrid composites.

It is difficult to compare the values of flexural strength and modulus obtained in this work to those

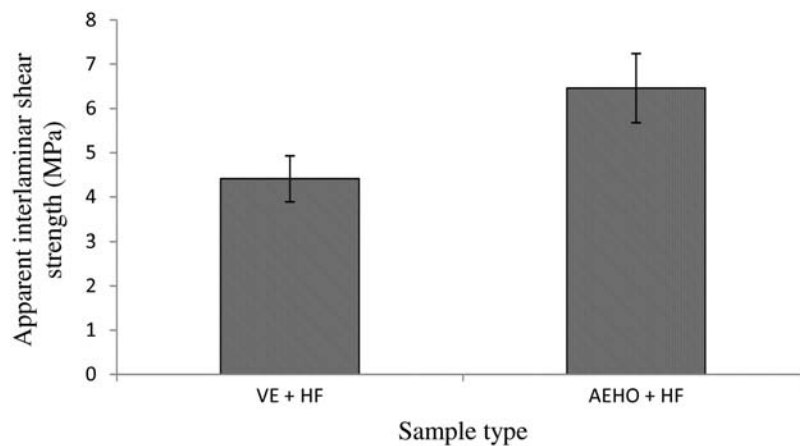


Figure 7. Interlaminar shear strength properties of AEHO-based hemp fiber biocomposite. AEHO: acrylated epoxidized hemp oil.

obtained by other researchers, since the reinforcement architecture, fiber volume fraction, manufacturing method and fiber and resin type are different. However, other researchers found the same decrease in the flexural properties of petrochemical matrices when natural fibers were added and hybrid composites were made. Wu et al.³⁹ reported that the flexural strength of PBT/Sisal composites decreased as the sisal content was increased, and attributed this behavior to the poor dispersion and compatibility between the fibers and the polymer. After grafting the PBT with acrylic acid, the authors reported that compatibility was improved and the flexural strength of the composites increased with the fiber volume fraction.

Figure 9 shows the flexural modulus of AEHO and VE resins as well as that of the biocomposites.

As expected, this property was found to be three times higher in the VE resin than in the bioresin sample. Accordingly this is due to the lower crosslink density and the long fatty acid chains of the AEHO. Considering the results found for the biocomposites, it can be seen that the addition of the hemp fiber mat improved the flexural modulus found for the matrices by 26% and 207% on VE and AEHO resins respectively. As a result, the biocomposite flexural modulus was just 23% lower than that of the hybrid composite.

Despite the flexural strength and elastic modulus of the VE resin being higher than the AEHO bioresin, no significant differences could be seen in the tensile behavior of the biocomposites and the hybrid composites, as shown in Figure 10. Although the mean values of tensile strength and tensile modulus are 5% lower for the

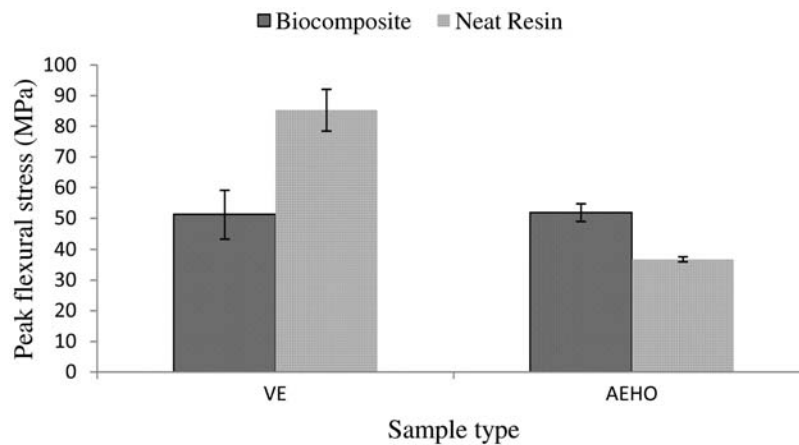


Figure 8. Peak flexural strength of AEHO-based bioresin and biocomposite samples. AEHO: acrylated epoxidized hemp oil.

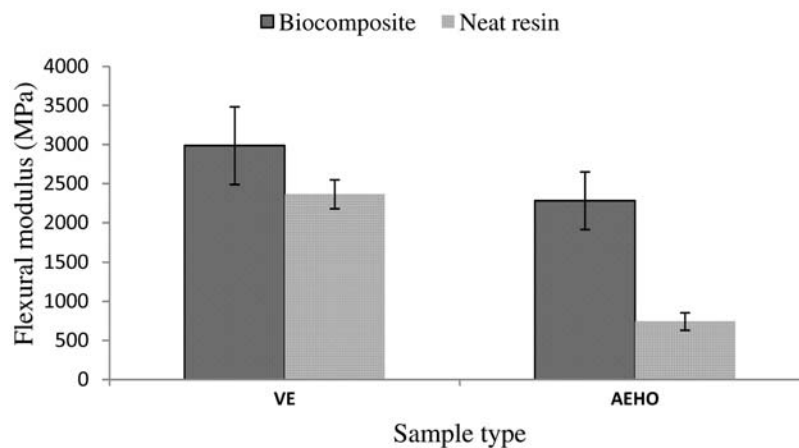


Figure 9. Flexural modulus of AEHO-based bioresin and biocomposite samples. AEHO: acrylated epoxidized hemp oil.

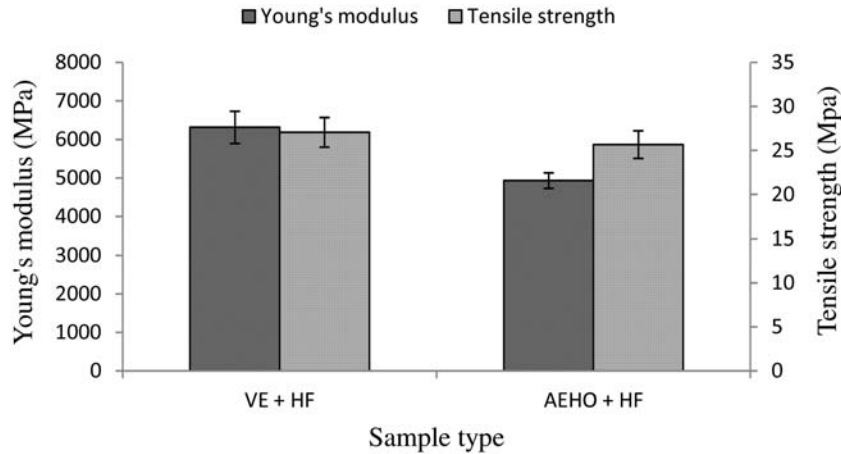


Figure 10. Tensile properties of AEHO-based biocomposite samples. AEHO: acrylated epoxidized hemp oil.

biocomposite, this difference falls within the error bars, thus no statement can be made regarding which sample type performs better in tensile behavior. The low compatibility of the hemp fibers with the VE resin is believed to be responsible for the low mechanical properties found in the hybrid composites, as seen previously in the flexural testing results. This incompatibility results in poor fiber/matrix adhesion, which means low load transfer from the matrix to the fibers and the presence of flaws (empty space between fiber and resin, as seen in the SEM images). Therefore this composite is essentially behaving like a flawed VE resin. On the other hand, the addition of hemp fiber reinforcement improves the properties of the bioresin, because these biocomposites present stronger fiber–matrix interfaces, as shown in the ILSS tests and SEM images. Consequently, the tensile behavior of hybrid composites and 100% hemp-based biocomposites is similar.

The values of tensile strength and modulus obtained in this work for VE and AEHO/hemp fiber mat composites are similar to those obtained by Mehta et al.⁴⁰ for polyester resin/hemp fiber mat (30 vol.%) compression molded hybrid composites. The authors could improve these properties significantly by performing different treatments on the hemp mat (alkali, silane, UPE–MEKP, and acrylonitrile) showing the importance of treating natural fiber reinforcements to obtain good mechanical performance on the hybrid composites. In addition, compression molded hybrid composites obtained by Mokhothu et al.⁴¹ and Wu et al.,³⁹ showed lower tensile properties than those of the neat resin.

Overall, mechanical properties found in this work for the hemp/VE hybrid composites are in accordance

to those reported by Ichhaporla⁴² for composite materials made of the same matrix and fiber type. The author characterized the properties in two directions since he used an orthotropic fabric, and reported the results for different web weights and needling punching passes. He found the flexural peak stress to be in the range 30–60 MPa and the tensile strength to be in the range 20–40 MPa, depending on the previously mentioned variables. Kim et al.⁴³ also studied the tensile properties of hemp/VE composites manufactured by the sheet molding compound technique. He found the elastic modulus to be similar to the one found in this work (3.1 GPa) but the tensile strength of the composites reported by the author was close to 100 MPa, which is four times higher than the one obtained in this work.

As with all mechanical properties, the impact strength of composite materials is dependent upon the properties of matrix and fibers as well as the properties of the interface between them. Usually, strong interfaces decrease the impact strength of composites since energy-consumption mechanisms such as fiber pull out are inhibited and the fracture occurs in a brittle manner. In a previous investigation,⁴⁴ the Charpy impact strength for different synthetic epoxy/bioresin (based on EHO and ESO) blends was studied. It was found that this property increased with increased bioresin concentration, which was attributed to the long fatty acid chains of the epoxidized vegetable oils imparting flexibility to the matrix thereby increasing the energy required to break the biocomposite samples. For this reason, the impact strength of the VE resin is expected to be lower than that of the AEHO-based bioresin, since the former is much less flexible, as shown in Figure 9. In contrast, it was

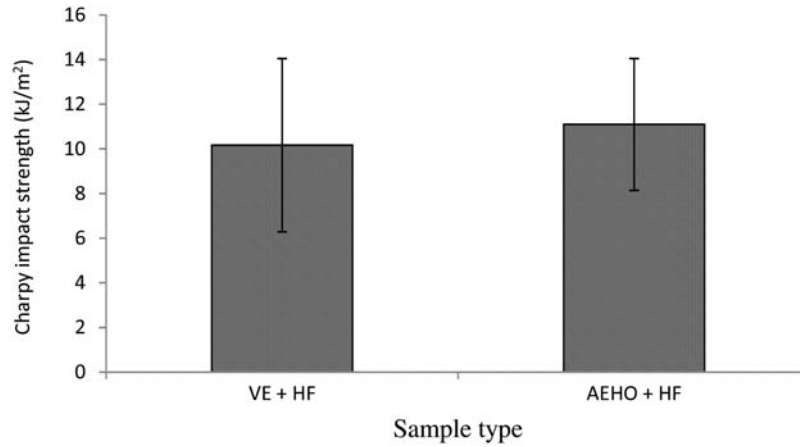


Figure 11. Charpy impact strength of AEHO-based biocomposite samples. AEHO: acrylated epoxidized hemp oil.

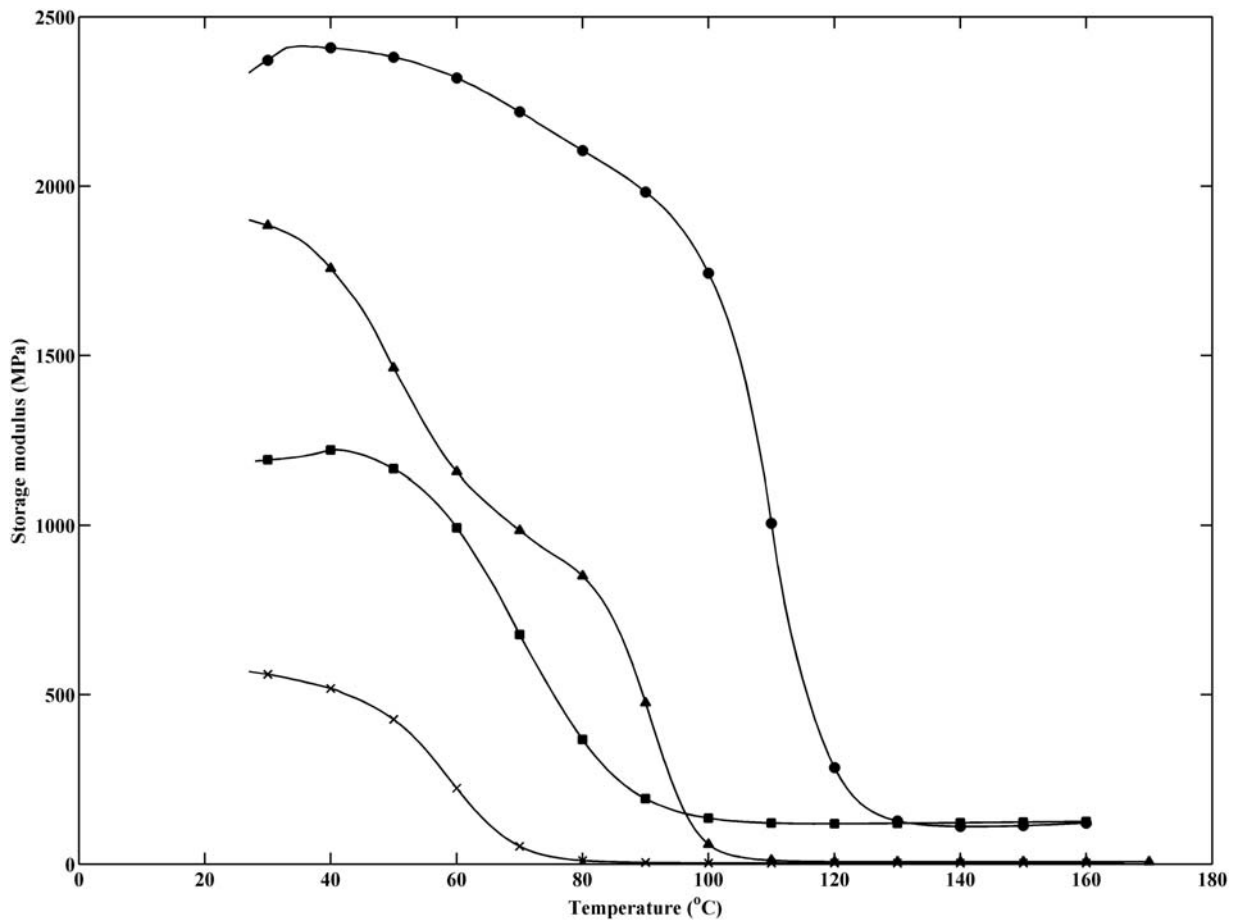


Figure 12. Storage modulus of AEHO-based bioresins and biocomposites. VE + HF (●), AEHO + HF (■), VE (▲) and AEHO (×). VE: vinyl ester; HF: hemp fiber; AEHO: acrylated epoxidized hemp oil.

apparent in all of the results presented previously in this work (ILSS, tensile, flexural and SEM images) than the interface between the hemp fibers and the bioresin is stronger than the interface with the

resin. These two opposite effects are theorized as being responsible for the impact properties of hybrid composites to be practically the same as in the 100% biocomposites (Figure 11).

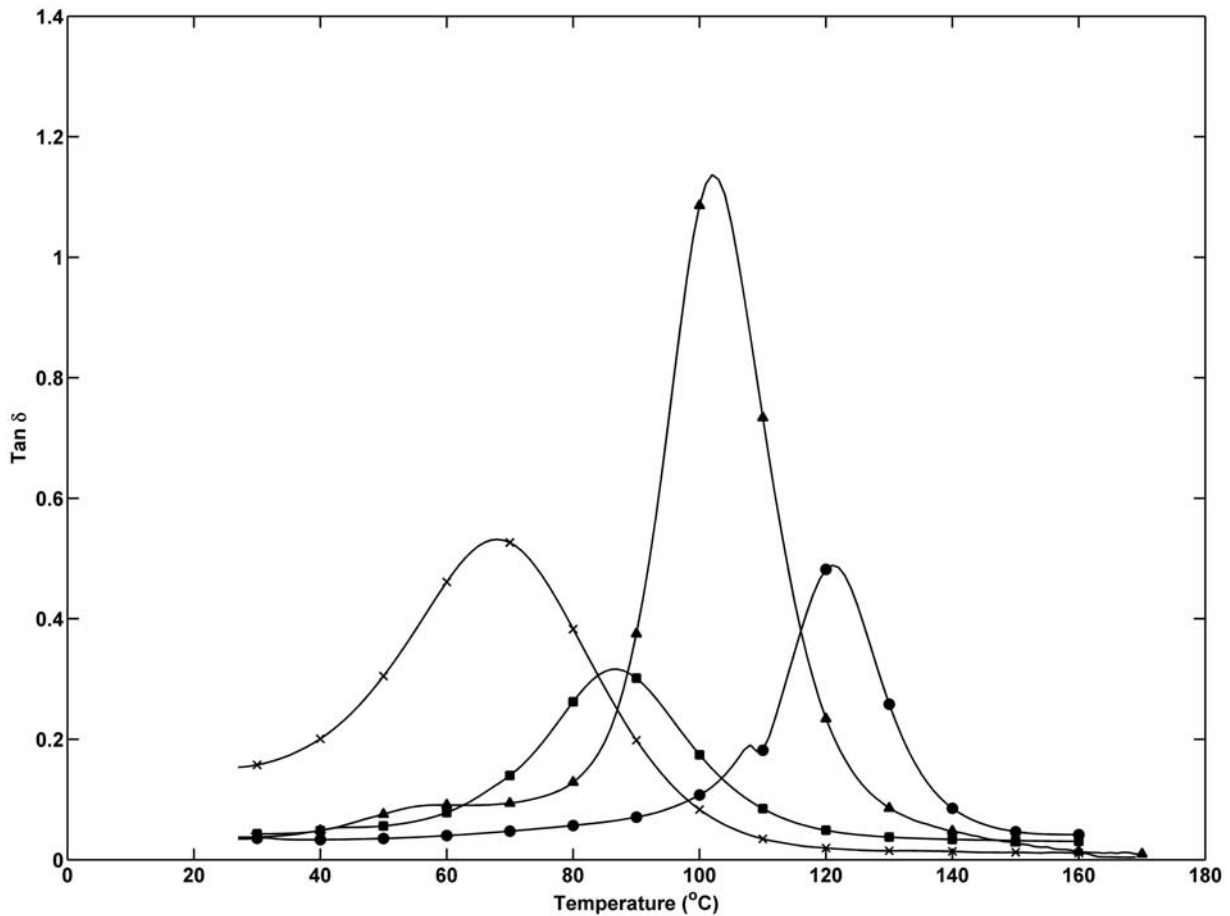


Figure 13. Tan δ of AEHO-based bioresins and biocomposites. VE + HF (\bullet), AEHO + HF (\blacksquare), VE (\blacktriangle) and AEHO (\times). VE: vinyl ester; HF: hemp fiber; AEHO: acrylated epoxidized hemp oil.

Dynamic mechanical properties

DMA was performed on bioresin and biocomposite samples in order to characterize the viscoelastic behavior of both VE- and AEHO-based neat bioresins and biocomposites. Figures 12 and 13 show the storage modulus plotted against temperature for the different bioresin and biocomposite samples. Table 1 summarizes the storage modulus at 40°C, T_g and crosslink density for both bioresin and biocomposite samples. As expected VE-based samples displayed higher storage modulus, T_g and crosslink density compared to AEHO-based samples. Fiber reinforcement served to increase storage modulus, T_g and crosslink density for both sample types. Specifically, the addition of hemp fiber reinforcement resulted in an improvement in storage modulus by factors of approximately 1.37 and 2.34 for the VE and AEHO samples, respectively. From examining Figure 13 it can be seen that the biocomposite samples have a less broad profile than those of the neat resin samples. Crosslink density was found to dramatically increase by factors of

Table 1. Dynamical mechanical properties of AEHO-based bioresins and biocomposites.

Sample type	Storage modulus at 40°C (MPa)	T_g (°C)	Crosslink density (mol/m ³)
Neat bioresin			
VE	1757	102	6654
AEHO	519	68	4301
Biocomposite			
VE + HF	2409	121	23,189
AEHO + HF	1216	87	22,885

VE: vinyl ester; HF: hemp fiber; AEHO: acrylated epoxidized hemp oil.

approximately 3.5 and 5.3 for the VE and AEHO samples, respectively.

Moisture absorption

Figure 14 displays the moisture absorption behavior for both VE and AEHO neat resin and hemp fiber

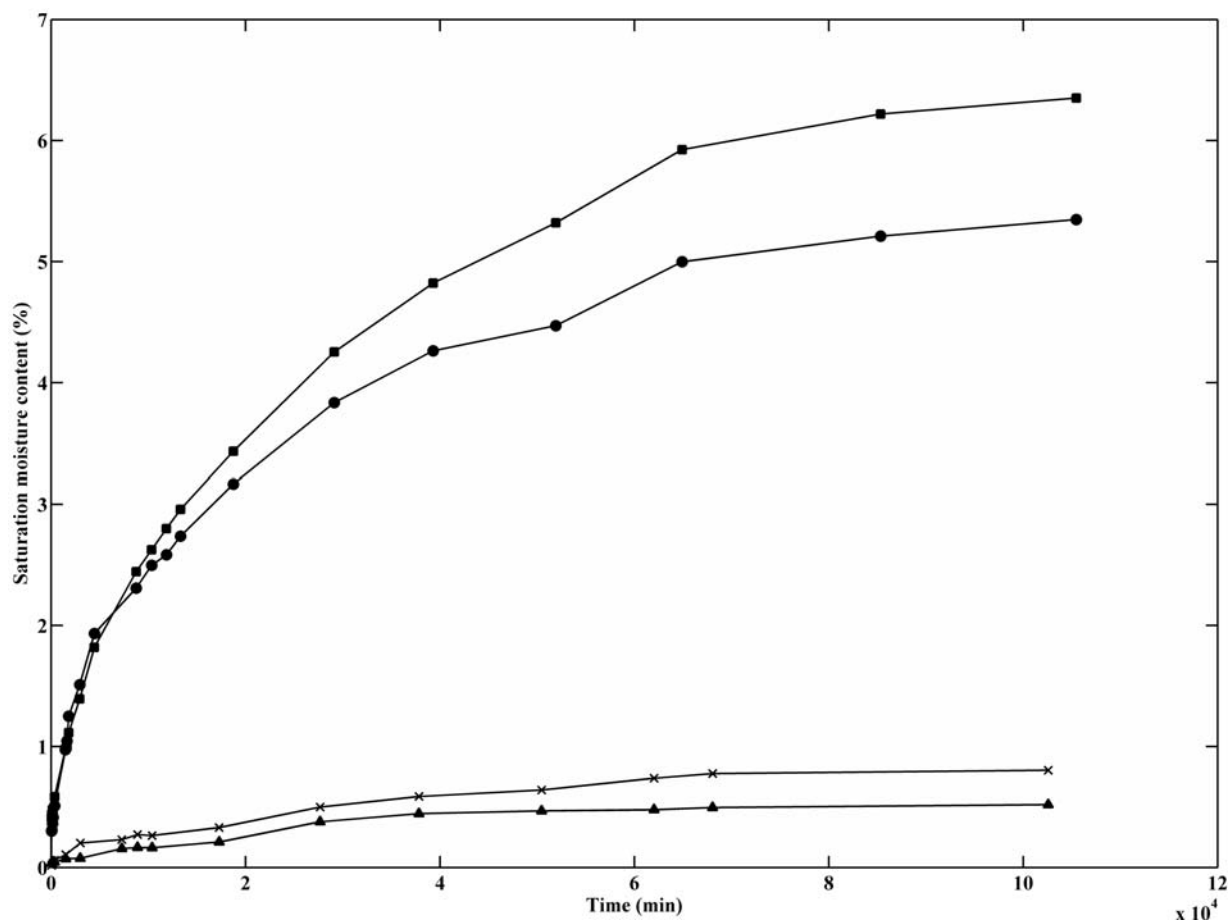


Figure 14. Water absorption properties of AEHO-based bioresins and biocomposites. VE + HF (●), AEHO + HF (■), VE (▲) and AEHO (×).

Table 2. Water absorption properties of AEHO-based bioresins and biocomposites. VE + HF (●), AEHO + HF (■), VE (▲) and AEHO (×).

Sample type	Diffusion coefficient $\times 10^{-6}$ (mm ² /s)	Saturation moisture content (%)
Bioresin samples		
VE	0.801	0.52
AEHO	0.958	0.80
Jute fiber samples		
VE	9.14	5.35
AEHO	9.68	6.35

VE: vinyl ester; HF: hemp fiber; AEHO: acrylated epoxidized hemp oil.

reinforced samples. Table 2 summarizes the diffusion coefficients and the saturation moisture content. It can be seen from the moisture absorption results that both the neat resin and biocomposite samples behaved consistent with a linear Fickian manner. After a rapid

moisture absorption phase the samples began to slow in absorption until equilibrium was reached. The transport mechanism was found to be heavily dominated by the fiber reinforcement. This is apparent from both Figure 14 and Table 2 whereby it can be seen that the both the diffusion coefficient and saturation moisture content are markedly higher for the biocomposite samples compared with those of the neat resin.

Conclusions

In this work, the mechanical performance (tensile, flexural, ILSS and impact) and the water absorption properties of 100% hemp-based biocomposite panels were investigated and compared to those of a VE hybrid composite. The test samples were cut from panels manufactured by the vacuum infusion technique, using a hemp fiber mat as reinforcement and two different matrices: a commercial VE resin and an AEHO-based bioresin synthesized in our laboratories.

Results showed that, except for the flexural modulus which was 23% higher in the case of the hybrid composite, no significant differences exist in the mechanical performance of both tested materials. The higher fiber/matrix compatibility of the biocomposites led to stronger fiber–matrix interfaces compensating the lower mechanical performance of the neat bioresin with respect to the VE. Therefore both biocomposites and hybrid composite showed to have practically the same flexural and tensile properties. Exactly the opposite happened in the impact tests, where the higher impact strength of the bioresin combined with the stronger fiber/matrix adhesion led to a composite material with similar impact strength than the one made with the VE resin, which has lower impact strength than the bioresin.

Moisture absorption tests showed that AEHO-based samples displayed both higher diffusion coefficient and saturation moisture content; however, fiber reinforcement was the dominant transfer mechanism. VE-based samples were found to display higher dynamical mechanical properties compared with AEHO-based samples. Storage modulus and crosslink density were found to drastically increase with the addition of hemp fiber reinforcement and as expected, T_g was also found to increase although to a lesser extent than the other properties.

This work showed that if no chemical treatments are performed on natural reinforcements, plant oil based bioresins (particularly if produced from the same source as the fiber reinforcement) should be used instead of petrochemical resins since the final properties are very similar in both type of composites, and the environmental impact would be reduced. As a future work, the effect of different fiber treatments on 100% biocomposites and hybrid composites is to be studied, to investigate the maximum mechanical properties that can be obtained in each case and see if the use of a petrochemical matrix is justified.

Acknowledgements

The authors would like to thank the Queensland State Government for providing a Smart Futures PhD Scholarship, and the Australian Government for providing an Endeavour Research Award. Thanks are also extended to Mr Wayne Crowell for providing technical support.

Conflict of interest

None declared.

Funding

This work was funded by the National Scientific and Technical Research Council of Argentina (CONICET).

References

1. Khot SN, Lascalea JJ, Can E, et al. Development and application of triglyceride-based polymers and composites. *J Appl Polym Sci* 2001; 82(3): 703–723.
2. Joshi SV, Drzal LT, Mohanty AK, et al. Are natural fiber composites environmentally superior to glass fiber reinforced composites? *Compos Part A: Appl Sci Manuf* 2004; 35(3): 371–376.
3. Francucci G, Rodríguez ES and Vázquez A. Study of saturated and unsaturated permeability in natural fiber fabrics. *Compos Part A: Appl Sci Manuf* 2010; 41(1): 16–21.
4. Rowell RM, Sanadi AR, Caulfield D, et al. Utilization of natural fibers in plastic composites: problems and opportunities. In: Leao AL, Carvalho FX and Frollini E (eds) *Lignocellulosic-plastics composites*. San Pablo: USP and UNESP, 1997, pp.23–51.
5. Akil HM, Cheng LW, Ishak ZAM, et al. Water absorption study on pultruded jute fibre reinforced unsaturated polyester composites. *Compos Sci Technol* 2009; 69: 1942–1948.
6. Sgriccia N, Hawley MC and Misra M. Characterization of natural fiber surfaces and natural fiber composites. *Compos Part A: Appl Sci Manuf* 2008; 39(10): 1632–1637.
7. Bledzki AK and Gassan J. Composites reinforced with cellulose based fibres. *Prog Polym Sci* 1999; 24(2): 221–274.
8. Thwea MM and Liaob K. Durability of bamboo-glass fiber reinforced polymer matrix hybrid composites. *Compos Sci Technol* 2003; 63: 375–387.
9. Bessadok A, Marais S, Gouanvé F, et al. Effect of chemical treatments of Alfa (*Stipa tenacissima*) fibres on water-sorption properties. *Compos Sci Technol* 2007; 67(3–4): 685–697.
10. Sreekala MS and Thomas S. Effect of fibre surface modification on water-sorption characteristics of oil palm fibres. *Compos Sci Technol* 2003; 63(6): 861–869.
11. Dhakal HN, Zhang ZY and Richardson MOW. Effect of water absorption on the mechanical properties of hemp fibre reinforced unsaturated polyester composites. *Compos Sci Technol* 2007; 67(7–8): 1674–1683.
12. Ahmed KS and Vijayarangan S. Experimental characterization of woven jute-fabric-reinforced isothalic polyester composites. *J Appl Polym Sci* 2007; 104: 2650–2662.
13. Bessadok A, Marais S, Roudesli S, et al. Influence of chemical modifications on water-sorption and mechanical properties of Agave fibres. *Compos Part A: Appl Sci Manuf* 2008; 39(1): 29–45.
14. Chen H, Miao M and Ding X. Influence of moisture absorption on the interfacial strength of bamboo/vinyl ester composites. *Compos Part A: Appl Sci Manuf* 2009; 40: 2013–2019.
15. Seki Y. Innovative multifunctional siloxane treatment of jute fiber surface and its effect on the mechanical properties of jute/thermoset composites. *Mater Sci Eng A* 2009; 508(1–2): 247–252.
16. Montazer M and Salehi A. Novel jute yarns grafted with methyl methacrylate. *J Appl Polym Sci* 2008; 107(4): 2067–2073.

17. Satheesh Kumar MN and Siddaramaiah. Water absorption behavior of acrylonitrile-butadiene (NBR) latex impregnated jute nonwoven fabric composites. *J Appl Polym Sci* 2006; 101(3): 2045–2050.
18. Francucci G, Rodriguez E and Vázquez A. Experimental study of the compaction response of jute fabrics in liquid composite molding processes. *J Compos Mater* 2012; 46(2): 155–167.
19. Ronga MZ, Zhangb MQ, Liub Y, et al. The effect of fiber treatment on the mechanical properties of unidirectional sisal-reinforced epoxy composites. *Compos Sci Technol* 2001; 61: 1437–1447.
20. Francucci G, Cardona F and Manthey NW. Cure kinetics of an acrylated epoxidized hemp oil-based bioresin system. *J Appl Polym Sci* 2013; (In press). DOI: 10.1002/app.38380.
21. Manthey NW, Cardona F, Francucci G, et al. Green building materials: hemp oil based biocomposites. In: *International conference on architectural and civil engineering 2012*, Bali, Indonesia, 24–25 October 2012, pp. 827–833.
22. Manthey MW, Cardona F, Aravinthan T, et al. Cure kinetics of an epoxidized hemp oil based bioresin system. *J Appl Polym Sci* 2011; 122(1): 444–451.
23. Manthey MW, Cardona F and Aravinthan T. Cure kinetic study of epoxidized hemp oil cured with a multiple catalytic system. *J Appl Polym Sci* 2012; 125(2): E511–E517.
24. Govignon Q, Bickerton S and Kelly P. Experimental investigation into the post-filling stage of the resin infusion process. *J Compos Mater* 2012; 47(12): 1479–1492.
25. Shabeer A, Chandrashekhara K and Schuman T. Synthesis and characterization of soy-based nanocomposites. *J Compos Mater* 2007; 41(15): 1825–1849.
26. Wambua P, Ivens J and Verpoest I. Natural fibres: can they replace glass in fibre reinforced plastics? *Compos Sci Technol* 2003; 63(9): 1259–1264.
27. Suardana NPG, Piao Y and Lim JK. Mechanical properties of hemp fibers and hemp/PP composites: effects of chemical surface treatment. *Mater Phys Mech* 2011; 11: 1–8.
28. Nabi Saheb D and Jog JP. Natural fiber polymer composites: a review. *Adv Polym Technol* 1999; 18(4): 351–363.
29. Miyagawa H, Mohanty A, Misra M, et al. Thermo-physical and impact properties of epoxy containing epoxidized linseed oil-amine-cured epoxy. *Macromol Mater Eng* 2004; 289(7): 636–641.
30. Morye SS and Wool RP. Mechanical properties of glass/flax hybrid composites based on a novel modified soybean oil matrix material. *Polym Compos* 2005; 26(4): 407–416.
31. Agarwal BD and Broutman LJ. *Analysis and performance of fiber composites*. New York: Wiley, 1990.
32. Halpin JC. *Primer on composite materials analysis*, 2nd ed. Boca Raton: CRC Press, 1992.
33. Kaw A. *Mechanics of composite materials*, 1st ed. Tampa, FL: CRC Press, 1997.
34. Reddy JN. *Mechanics of composite materials and shells-theory and analysis*. Boca Raton: CRC Press, 2003.
35. Wright WW. *Design with advanced composite materials*. Berlin, Heidelberg, London: Springer Verlag, 1989.
36. Petker I. The influence of resin strength and defects on the interlaminar shear strength of filament-wound composites. *Polym Eng Sci* 1965; 5(1): 49–58.
37. Dhakal HN, Zhang ZY, Richardson MOW, et al. The low velocity impact response of non-woven hemp fibre reinforced unsaturated polyester composites. *Compos Struct* 2007; 81(4): 559–567.
38. Zini E and Scandola M. Green composites: an overview. *Polym Compos* 2011; 32(12): 1905–1915.
39. Wu C-S, Yen F-S and Wang C-Y. Polyester/natural fiber biocomposites: preparation, characterization, and biodegradability. *Polym Bull* 2011; 67(8): 1605–1619.
40. Mehta G, Drzal LT, Mohanty AK, et al. Effect of fiber surface treatment on the properties of biocomposites from nonwoven industrial hemp fiber mats and unsaturated polyester resin. *J Appl Polym Sci* 2006; 99(3): 1055–1068.
41. Mokhothu TH, Guduri BR and Luyt AS. Kenaf fiber-reinforced copolyester biocomposites. *Polym Compos* 2011; 32(12): 2001–2009.
42. Ichhaporia PK. *Composites from natural fibers*, Proquest: Umi Dissertation Publishing, pp.87–97.
43. Kim W, Argento A, Lee E, et al. High strain-rate behavior of natural fiber reinforced polymer composites. *J Compos Mater* 2011; 46(9): 1051–1065.
44. Manthey NW, Cardona F and Aravinthan T. Mechanical properties of epoxidized hemp oil based biocomposites: preliminary results. In: *The first international postgraduate conference on engineering, Designing and developing the built environment for sustainable wellbeing*, 28 April 2011. Brisbane, Queensland: Queensland University of Technology.